Structural Engineering and Mechanics, Vol. 44, No. 5 (2012) 681-704
DOI: http://dx.doi.org/10.12989/sem.2012.44.5.681

Dynamic response of Euler-Bernoulli beams to resonant harmonic moving loads

Giuseppe Piccardo[a] and Federica Tubino*

DICCA, University of Genoa, Via Montallegro 1, 16145 Genoa, Italy

(Received November 3, 2011, Revised October 30, 2012, Accepted November 9, 2012)

Abstract. The dynamic response of Euler-Bernoulli beams to resonant harmonic moving loads is analysed. The non-dimensional form of the motion equation of a beam crossed by a moving harmonic load is solved through a perturbation technique based on a two-scale temporal expansion, which permits a straightforward interpretation of the analytical solution. The dynamic response is expressed through a harmonic function slowly modulated in time, and the maximum dynamic response is identified with the maximum of the slow-varying amplitude. In case of ideal Euler-Bernoulli beams with elastic rotational springs at the support points, starting from analytical expressions for eigenfunctions, closed form solutions for the time-history of the dynamic response and for its maximum value are provided. Two dynamic factors are discussed: the Dynamic Amplification Factor, function of the non-dimensional speed parameter and of the structural damping ratio, and the Transition Deamplification Factor, function of the sole ratio between the two non-dimensional parameters. The influence of the involved parameters on the dynamic amplification is discussed within a general framework. The proposed procedure appears effective also in assessing the maximum response of real bridges characterized by numerically-estimated mode shapes, without requiring burdensome step-by-step dynamic analyses.

Keywords: closed form solution; Euler-Bernoulli beams; harmonic moving loads; vibrations

1. Introduction

The analysis of simple Euler-Bernoulli beams crossed by harmonic loads is of interest both from a theoretical point of view, with the aim of assessing the influence of the involved parameters on the dynamics, and from a technical point of view, in order to provide efficient tools to estimate easily the maximum dynamic response and the dynamic amplification factor. Moving harmonic loads can represent, for instance, a component of the load transmitted to rails by moving trains (Fryba 1999, Garinei 2006), the load applied by vehicles resulting from the pavement surface roughness and the mechanical systems of the vehicle (Kim 2004), or the load exerted on a footbridge by a walking pedestrian (Allen and Murray 1993, Bachmann *et al.* 1995).

The monograph by Fryba (1999), containing a large body of work on moving load problems and providing an extensive bibliography (up to the nineties) in this field, reports a closed-form solution for the dynamic response of a simply-supported beam crossed by a moving resonant harmonic load.

*Corresponding author, Assistant Professor, E-mail: federica.tubino@unige.it
[a]Associate Professor, E-mail: giuseppe.piccardo@unige.it

The dynamic response of beams to harmonic moving loads has been recently analysed within different contexts: railway engineering (e.g., Chen *et al.* 2001, Kargarnovin 2005), beam-type dynamic absorber (e.g., Oniszczuk 2003), dynamic response of pavement systems to vehicles (e.g., Kim 2004), pre-stressed beams of viaducts in roadways, railways and bridges (e.g., Kocaturk and Simsek 2006). All such studies, involving the modelling of the soil, the presence of axial loads and the modelling of connected beams, describe parametric analyses showing the time-history of the dynamic response for different values of the parameters governing the dynamics of the problem (commonly, velocity and frequency of the load).

The vibrations of simple beam-like modelled bridges crossed by a moving harmonic load have been recently re-examined, within railway engineering applications (Abu-Hilal and Mosen 2000, Garinei 2006, Garinei and Risitano 2008). In these papers, based on the closed-form solution of the convolution integral, complicated analytical expressions for the dynamic response are provided; furthermore, parametric analyses are performed for different values of the involved parameters. Catal (2012) has recently studied the forced vibration of Euler-Bernoulli beams using the differential transform method. Starting from the classic closed form solution for the dynamic response of a simply-supported beam crossed by a resonant harmonic moving load proposed by Fryba (1999), Pimentel and Fernandes (2002) performed numerical simulations to evaluate the maximum pedestrian-induced dynamic response of footbridges for various values of the damping ratio. The main limit of the papers in the literature is the lack of a general framework in order to assess the role of the involved parameters. The authors of the present paper have analyzed the dynamic response of simply-supported beams to resonant moving harmonic loads (Tubino and Piccardo 2008, Piccardo and Tubino 2009), providing closed-form solutions for the dynamic response and for the dynamic amplification factor as functions of suitably-defined non-dimensional parameters. Moreover, concerning the case of relatively slow motion (typical of pedestrian-induced loads), they represent the dynamic response as a harmonic modulate in time by slowly-varying amplitudes. Ricciardelli and Briatico (2011) have proposed a solution conceptually very similar to Tubino and Piccardo (2008), Piccardo and Tubino (2009), using a different non-dimensional form. They achieve results in perfect accordance with Tubino and Piccardo (2008), Piccardo and Tubino (2009), as regards the resonant condition; furthermore, they discuss the possibility of obtaining approximate solutions away from resonance.

In this paper, a general approach is proposed for evaluating the dynamic response of a generic Euler-Bernoulli beam, provided with rotational springs at both ends, to resonant harmonic moving loads in order to achieve simple closed-form expressions for the dynamic response and for the dynamic amplification factor. The problem can generally be solved by the convolution integral, which can be estimated in closed-form if the mode shape is expressed through a simple analytical expression (e.g., Abu-Hilal and Mosen 2000, Garinei 2006), or numerically if the mode shape is more complicated. The non-dimensional form of the equation of motion and the ordering of the governing parameters, according to their technical values, point out that the forcing function can be expressed as the product of two terms depending on two different (slow and fast) time scales. Such a particular condition suggests the possibility of solving the equation of motion through a perturbation technique based on a two temporal scale expansion, able to represent the solution as a harmonic function slowly modulated in time (two-variable expansion procedure; Kevorkian and Cole 1996, Simmonds and Mann 1998, Nayfeh and Mook 1979); thus, the maximum dynamic response coincides with the maximum of the slow-variable amplitude. Furthermore, based on a closed-form expression of the mode shapes for a generic Euler-Bernoulli beam, equipped with

rotational springs at both ends and fixed vertical supports (Appendix A), analytical expressions of the response amplitude and of the dynamic amplification factor can be deduced as a function of a suitable non-dimensional speed parameter (depending on the structural properties - span length and circular natural frequency - and on the load velocity; Fryba 1999) and of the structural damping ratio.

In Section 2 the vibrations of a beam to a moving harmonic load are analysed adopting both the convolution integral and the two-scale perturbation technique, showing that the dynamic response can be schematized as a harmonic with slow-varying amplitude. In Section 3, based on the analytical expression for mode shapes of Euler-Bernoulli beams with different boundary conditions, closed-form solutions are obtained for the response amplitude, the Dynamic Amplification Factor (i.e., the ratio between the maximum dynamic response and the static response to the maximum dynamic load) and the Transition Deamplification Factor (i.e., the ratio between the effective maximum dynamic response and the maximum dynamic response to the harmonic load fixed in the point where the eigenfunction is maximum), as functions of suitable non-dimensional parameters. In particular cases (Section 3.1-3.2) as simply-supported and double-clamped beams, the proposed solution becomes particularly simple and permits to recognize literature solutions and their limits of applicability. Numerical examples of ideal and real beams showing the consistency of the proposed formulation are given in Section 4. Finally, some conclusions are drawn (Section 5).

2. Mathematical formulation

The deflection $q(x,t)$ of a Euler-Bernoulli prismatic beam to a harmonic load moving with a constant speed c (Fig. 1) is described by the well-known field equation

$$\mu\frac{\partial^2 q(x,t)}{\partial t^2}+\chi\frac{\partial q(x,t)}{\partial t}+EJ\frac{\partial^4 q(x,t)}{\partial x^4}=F_0\sin(\Omega t)\delta(x-ct)[H(t)-H(t-L/c)] \tag{1}$$

where μ is the mass per unit length, χ is the damping coefficient, EJ is the flexural stiffness, F_0 and Ω are, respectively, the amplitude and the circular frequency of the moving load, δ is the Dirac delta function, H is the Heaviside step function, L is the beam span length.

By the standard Galerkin method, the solution of Eq. (1) can be expressed in the form

$$q(x,t)=\sum_{j=1}^{N}\varphi_j(x)p_j(t) \tag{2}$$

where $\varphi_j(x)$ is the j-th comparison function (Meirovitch 1980) and $p_j(t)$ is the corresponding

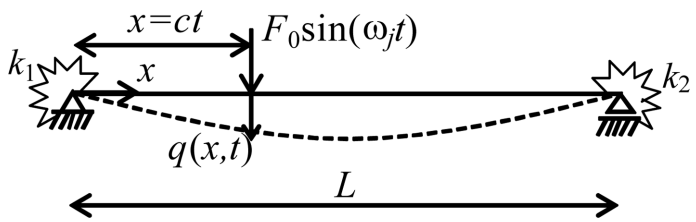

Fig. 1 Schematic representation of a generic beam crossed by a harmonic load

principal (or generalized) coordinate. By using the eigenfunctions of the eigenvalue problem related to the free response of Eq. (1), $\varphi_j(x)$ is assumed as the j-th vibration mode of the beam and, being a comparison function, it satisfies the mechanical and geometric boundary conditions of the beam (Fig. 1; Appendix A). Thanks to the orthogonality property of eigenfunctions, assuming proportional damping, the equation of motion of the j-th principal coordinate p_j is

$$\ddot{p}_j(t) + 2\xi_j\omega_j\dot{p}_j(t) + \omega_j^2 p_j(t) = \frac{1}{M_j}F_j(t) \tag{3}$$

where ξ_j is the modal damping ratio, ω_j is the natural circular frequency, M_j is the modal mass, $F_j(t)$ is the modal force. Expressing the generic mode shape φ_j as a function of a non-dimensional abscissa $\zeta = x/L$, $F_j(t)$ is given by

$$F_j(t) = \sin(\Omega t)\varphi_j\left(\frac{ct}{L}\right)[H(t) - H(t - L/c)] \tag{4}$$

Let us introduce the following non-dimensional quantities

$$\tilde{t} = \omega_j t \qquad \tilde{p}_j = \frac{p_j}{L} \qquad \tilde{\Omega} = \frac{\Omega}{\omega_j} \qquad \tilde{\Omega}_c = \frac{c}{\omega_j L} \qquad \varepsilon = \frac{F_0}{M_j\omega_j^2 L} \tag{5}$$

where $\tilde{\Omega}$ is the non-dimensional frequency and $\tilde{\Omega}_c$ is the non-dimensional speed parameter (Fryba 1999). The coefficient ε is considered as a naturally small parameter, assuming F_0 much lower than the product $M_j\omega_j^2 L$. Substituting Eqs. (4) and (5) into Eq. (3), it becomes

$$\ddot{\tilde{p}}_j + 2\xi_j\dot{\tilde{p}}_j + \tilde{p}_j = \varepsilon\sin(\tilde{\Omega}\tilde{t})\varphi_j(\tilde{\Omega}_c\tilde{t})\left[H(\tilde{t}) - H(1/\tilde{\Omega}_c)\right] \tag{6}$$

Since the structural damping is usually small too, and assuming the non-dimensional speed parameter $\tilde{\Omega}_c$ equally small (such an assumption is valid if c is small compared with the product $\omega_j L$, namely the speed of the harmonic load is sufficiently lower than the critical speed of the beam), they can be expressed as small of the same order of the parameter ε

$$\xi_j = \varepsilon\xi^* \qquad \tilde{\Omega}_c = \varepsilon\Omega_c^* \tag{7}$$

The limit of validity of this assumption on the non-dimensional speed parameter will be deeply discussed in Section 3.

Substituting Eq. (7) into Eq. (6), it becomes

$$\ddot{\tilde{p}}_j + 2\varepsilon\xi^*\dot{\tilde{p}}_j + \tilde{p}_j = \varepsilon\sin(\tilde{\Omega}\tilde{t})\varphi_j(\varepsilon\Omega_c^*\tilde{t})[H(\tilde{t}) - H(1/\varepsilon\tilde{\Omega}_c)] \tag{8}$$

The solution of Eq. (8) can be easily expressed through the convolution integral, which in general has to be solved numerically for a generic structural mode. However, the non-dimensional form points out the particular expression of the forcing function, being the product of a sinusoidal term, depending on the non-dimensional time $\tilde{t}$, and of the structural mode shape, depending on a slower time scale $\varepsilon\tilde{t}$. Such a particular condition suggests the possibility of solving Eq. (8) through a perturbation technique based on a two-scale expansion (Kevorkian and Cole 1996, Simmonds and Mann 1998), that can be seen as an application of the Multiple Scale Method (MSM) (e.g., Nayfeh

and Mook 1979) using two sole temporal scale. The (perhaps) unusual adoption of the MSM for solving a simple linear dynamic problem allows us to represent the solution as a harmonic function slowly modulated in time; such an expression permits an easy determination of the maximum value of the response, which can be very useful for practical applications. In the following, both the solutions through the convolution integral (Section 2.1) and through the two-scale perturbation technique (Section 2.2) will be presented. Finally, considerations about the dynamic response and its maximum value are reported in Section 2.3.

2.1 Solution by the convolution integral

Eq. (8) can be solved through the convolution integral (e.g., Clough and Penzien 2003)

$$\tilde{p}(\tilde{t}) = \varepsilon \int_0^{\tilde{t}} \sin(\tilde{\Omega}\tilde{\tau})\varphi_j(\varepsilon\Omega_c^*\tilde{\tau})\tilde{h}(\tilde{t}-\tilde{\tau})d\tilde{\tau} \tag{9}$$

where $\tilde{h}(\tilde{t})$ is the non-dimensional impulse response function of the *j*-th mode of vibration

$$\tilde{h}(\tilde{t}) = \frac{1}{\sqrt{1-\varepsilon^2\xi^{*2}}}\exp(-\varepsilon\xi^*\tilde{t})\sin(\sqrt{1-\varepsilon^2\xi^{*2}}\tilde{t}) \simeq \exp(-\varepsilon\xi^*\tilde{t})\sin(\tilde{t}) \tag{10}$$

neglecting the terms of order $O(\varepsilon^2)$.

Substituting Eq. (10) into Eq. (9) and taking into account suitable trigonometric identities, one obtains

$$\tilde{p}(\tilde{t}) = \varepsilon\exp(-\varepsilon\xi^*\tilde{t})\left\{\begin{array}{l}\left[\int_0^{\tilde{t}} \sin(\tilde{\Omega}\tilde{\tau})\varphi_j(\varepsilon\Omega_c^*\tilde{\tau})\exp(\xi^*\tilde{\tau})\cos(\tilde{\tau})d\tilde{\tau}\right]\sin(\tilde{t}) + \\ -\left[\int_0^{\tilde{t}} \sin(\tilde{\Omega}\tilde{\tau})\varphi_j(\varepsilon\Omega_c^*\tilde{\tau})\exp(\xi^*\tilde{\tau})\sin(\tilde{\tau})d\tilde{\tau}\right]\cos(\tilde{t})\end{array}\right\} \tag{11}$$

Under the hypothesis that $\tilde{\Omega} = 1$ (i.e., perfect resonance), Eq. (11) can be rewritten as follows

$$\tilde{p}(\tilde{t}) = \varepsilon\exp(-\varepsilon\xi^*\tilde{t})\left\{\begin{array}{l}-\left[\frac{1}{2}\int_0^{\tilde{t}} \varphi_j(\varepsilon\Omega_c^*\tilde{\tau})\exp(\varepsilon\xi^*\tilde{\tau})d\tilde{\tau}\right]\cos(\tilde{t}) + \\ +\left[\frac{1}{2}\int_0^{\tilde{t}} \sin(2\tilde{\tau})\varphi_j(\varepsilon\Omega_c^*\tilde{\tau})\exp(\varepsilon\xi^*\tilde{\tau})d\tilde{\tau}\right]\sin(\tilde{t}) + \\ +\left[\frac{1}{2}\int_0^{\tilde{t}} \cos(2\tilde{\tau})\varphi_j(\varepsilon\Omega_c^*\tilde{\tau})\exp(\varepsilon\xi^*\tilde{\tau})d\tilde{\tau}\right]\cos(\tilde{t})\end{array}\right\} \tag{12}$$

Therefore, the dynamic response evaluated by the convolution integral, Eq. (9), can be expressed as the summation of three integrals: the first one depends on a non-oscillating function through the slower time scale $\varepsilon\tilde{\tau}$, while the second and third integrands are oscillating functions depending on the fast time scale $\tilde{\tau}$. The solution of Eq. (12) leads to the exact dynamic response of the system, and it can be evaluated in closed-form only for particular expressions of the mode shape φ_j.

2.2 Solution by the two-scale perturbation method

The particular expression of the forcing term in Eq. (8) suggests the possibility of solving it through a perturbation method based on a temporal scale expansion, introducing the two time scales $\tilde{t}_0 = \tilde{t}$ and $\tilde{t}_1 = \varepsilon\tilde{t}$ (two-variable expansion or two-scale method), so that the first and second time-derivative are expressed as $d/d\tilde{t} = D_0 + \varepsilon D_1$, and $d^2/d\tilde{t}^2 = D_0^2 + 2\varepsilon D_0 D_1$, where $D_j = \partial/\partial\tilde{t}_j$ (j = 0, 1).

The solution $\tilde{p}_j$ can be developed in series of the small parameter $\varepsilon \ll 1$

$$\tilde{p}_j = \tilde{p}_0 + \varepsilon\tilde{p}_1 + \ldots \tag{13}$$

Substituting Eq. (13) into Eq. (8) and equating the coefficients at the same order of ε, the two following perturbation equations are obtained (up to order ε)

Order ε^0 $$D_0^2[\tilde{p}_0] + \tilde{p}_0 = 0 \tag{14}$$

Order ε $$D_0^2[\tilde{p}_1] + \tilde{p}_1 = -2D_0D_1[\tilde{p}_0] - 2\xi_j^* D_0[\tilde{p}_0] + \sin(\tilde{\Omega}\tilde{t}_0)\varphi_j(\Omega_c^*\tilde{t}_1) \tag{15}$$

The general solution of Eq. (14) is given by

$$\tilde{p}_0 = A(\tilde{t}_1)\exp(i\tilde{t}_0) + c.c. \tag{16}$$

where i is the imaginary unit and the term *c.c.* denotes the complex conjugate.

Substituting Eq. (16) into Eq. (15), it becomes

$$D_0^2[\tilde{p}_1] + \tilde{p}_1 = -2i\frac{\partial A(\tilde{t}_1)}{\partial\tilde{t}_1}\exp(i\tilde{t}_0) - 2\xi_j^* iA(\tilde{t}_1)\exp(i\tilde{t}_0) + \frac{1}{2i}\exp(i\tilde{\Omega}\tilde{t}_0)\varphi_j(\Omega_c^*\tilde{t}_1) + c.c. \tag{17}$$

Under the particular condition of perfect resonance, $\tilde{\Omega} = 1$ (i.e., the loading frequency is perfectly coincident with the structural frequency), corresponding to the maximum dynamic structural response, Eq. (17) becomes

$$D_0^2[\tilde{p}_1] + \tilde{p}_1 = \left[-2i\frac{\partial A(\tilde{t}_1)}{\partial\tilde{t}_1} - 2\xi_j^* iA(\tilde{t}_1) + \frac{1}{2\mathrm{i}}\varphi_j(\Omega_c^*\tilde{t}_1)\right]\exp(i\tilde{t}_0) + c.c. \tag{18}$$

Eliminating the term that produces a secular term in $\tilde{p}_1$ demands that

$$\frac{\partial A(\tilde{t}_1)}{\partial\tilde{t}_1} + \xi_j^* A(\tilde{t}_1) = -\frac{1}{4}\varphi_j(\Omega_c^*\tilde{t}_1) \tag{19}$$

which leads to

$$A(\tilde{t}_1) = -\frac{1}{4}\int_0^{\tilde{t}_1}\varphi_j(\Omega_c^*\tau)\exp\left[-\xi_j^*(\tilde{t}_1 - \tau)\right]d\tau \tag{20}$$

It is evident from Eq. (20) that A is a real function, thus Eq. (16) can simply be re-written as

$$\tilde{p}_0 = 2A(\tilde{t}_1)\cos(\tilde{t}_0) \tag{21}$$

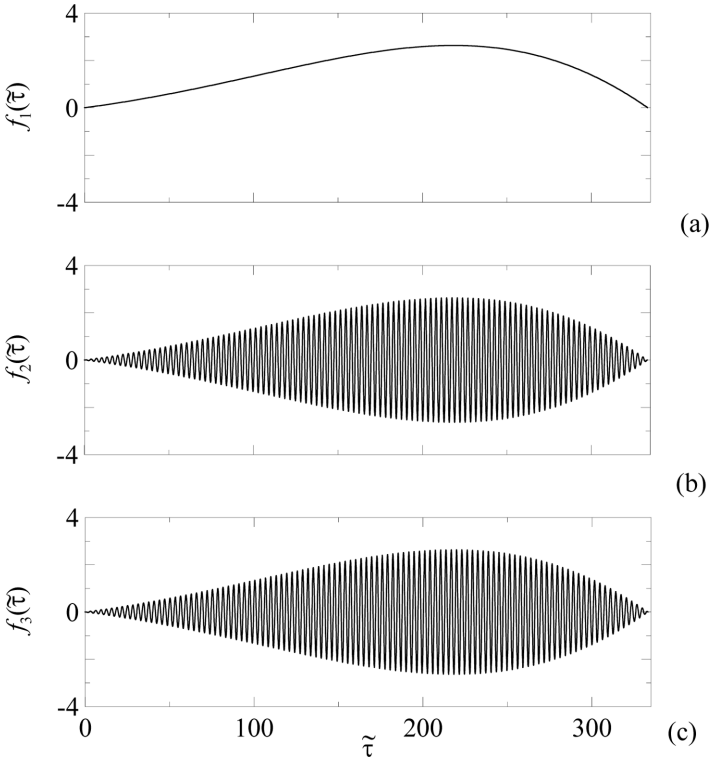

Fig. 2 Typical picture of the three integrands in Eq. (12) ($\tilde{\Omega}_c = 0.003$, $\xi_j = 0.005$), being $f_1(\tilde{\tau}) = \varphi_j(\tilde{\Omega}_c\tilde{\tau})\exp(\xi_c\tilde{\tau})$, $f_2(\tilde{\tau}) = \sin(2\tilde{\tau})\varphi_j(\tilde{\Omega}_c\tilde{\tau})\exp(\xi_j\tilde{\tau})$, $f_3(\tilde{\tau}) = \cos(2\tilde{\tau})\varphi_j(\Omega_c\tilde{\tau})\exp(\xi_j\tilde{\tau})$

Substituting Eq. (20) into Eq. (21), the solution $\tilde{p}_j$ is obtained (at the first approximation order)

$$\tilde{p}_j(\tilde{t}) = -\frac{\varepsilon}{2}\left[\int_0^{\tilde{t}_1}\varphi_j(\Omega_c^*\tau)\exp(\xi_j^*\tau)d\tau\right]\exp(-\xi_j^*\tilde{t}_1)\cos(\tilde{t}_0) \tag{22}$$

Eq. (22) coincides with the first term of the exact solution (12), obtained through the convolution integral. It can be observed that all the integrands at the right-hand side of Eq. (12) involve the same expression depending on the slow time-scale, but the second and third ones are also multiplied by a function of the fast time-scale. As a consequence, the second and third integrals in Eq. (12), calculated on functions fast oscillating in time, are very small compared to the first integral (the only one retained by the perturbation method) calculated on the slowly variable function. Fig. 2 shows a picture of the three integrands in the particular case of sinusoidal mode of vibration; in general, their shape depends on the non-dimensional parameters $\tilde{\Omega}_c$ and ξ_j, and on the mode $\varphi_j(x)$. It has been verified that the qualitative trend of such functions does not noticeably modify when other mode shapes or different structural parameters are considered.

2.3 Dynamic response and corresponding maximum value

From Eq. (22) the j-th principal coordinate $p_j(\tilde{t})$ can be expressed in the following meaningful way

$$p_j(\tilde{t}) = A_j(\tilde{t})\cos(\tilde{t}) \tag{23}$$

where $A_j(\tilde{t})$ is the dimensional slow-varying amplitude

$$A_j(\tilde{t}) = -\frac{F_0}{2M_j\omega_j^2}\left[\int_0^{\tilde{t}}\varphi_j(\tilde{\Omega}_c\tilde{\tau})\exp(\xi_j\tilde{\tau})d\tilde{\tau}\right]\exp(-\xi_j\tilde{t}) \tag{24}$$

It should be noted that this integral can be easily approximated by a summation if the vibration mode is not known in closed form (Tubino and Piccardo 2008). Therefore Eq. (24) can be employed to evaluate the amplitude of the dynamic response of a generic structure (modeled as a 1-D continuum) to a resonant harmonic moving load (see Section 4.2).

Under the simplifying hypothesis that the beam dynamic response is dominated by the j-th resonant mode of vibration, the structural response in terms of displacement and acceleration can be approximated by the following equations

$$\begin{aligned} q(\zeta,\tilde{t}) &\simeq \varphi_j(\zeta)A_j(\tilde{t})\cos(\tilde{t}) \\ \ddot{q}(\zeta,\tilde{t}) &\simeq -\varphi_j(\zeta)A_j(\tilde{t})\cos(\tilde{t}) \end{aligned} \tag{25}$$

ζ being the non-dimensional abscissa, x/L.

The Dynamic Amplification Factor (DAF) is usually defined as the ratio between the effective maximum dynamic response (hence in the point where the structural eigenfunction is maximum) and the maximum static response (i.e., the static response to the maximum value of the dynamic load applied in the point where the structural eigenfunction is maximum). Being the dynamic response expressed by Eq. (25), the maximum dynamic response is proportional to the maximum amplitude $A_{j\max} = \max[|A_j(\tilde{t})|]$; thus, the DAF can be expressed as

$$\beta = \frac{A_{j\max}M_j\omega_j^2}{F_0\left|\varphi_j\right|_{\max}} = \beta(\tilde{\Omega}_c,\xi_j) \tag{26}$$

where $|\varphi_j|_{\max}$ is the maximum value of the modulus of the beam mode shape, $|\varphi_j|_{\max} = \max[|\varphi_j(\tilde{x})|]$. It is evident that the factor β depends on the non-dimensional parameters $\tilde{\Omega}_c$ and ξ_j through the maximum amplitude $A_{j\max}$; it assumes values much greater than 1, of the order of $1/(2\xi_j)$, if the load velocity is very small.

Furthermore, a Transition Deamplification Factor (TDF) β^* can be introduced as the ratio between the effective maximum dynamic response to a moving resonant harmonic load and the maximum dynamic response to the same load considered fixed in the point where the structural eigenfunction is maximum. Thus, the TDF β^* expresses the reduction in the maximum dynamic response due to the effect of the motion of the load, and it can be formulated as a function of the DAF β as follows

$$\beta^* = \beta\cdot 2\xi_j = \beta^*(\tilde{\Omega}_c/\xi_j) \tag{27}$$

For its definition, the TDF β^* is always lower than unity and it has the advantage of formally depending from only one parameter, the ratio $\tilde{\Omega}_c/\xi_j$: such a circumstance is expressly clarified in Section 3, where the problem is solved in closed-form for ideal beams. Nevertheless, the classic

DAF definition maintains its usefulness since it points out the limits of applicability of the proposed solution (essentially depending on values of the non-dimensional speed parameter $\tilde{\Omega}_c$), which are not explicit in the TDF expression.

3. Closed-form solution for ideal beams

For simple structural schemes, analytical expressions are available for the mode shape φ_j: in such cases, the integral in Eq. (24) can be solved in closed-form. Furthermore, the maximum value of the amplitude of the j-th principal coordinate, and thus the DAF β and the TDF β^*, can be expressed in closed-form as a function of the non-dimensional parameters.

Let us consider a Euler-Bernoulli beam, with two rotational springs of different stiffness k_1 and k_2 at the right and left end, respectively (Fig. 1). The following j-th mode shape can be assumed for generic boundary conditions (see Appendix A)

$$\varphi_j(x) = \frac{2\lambda_j}{\alpha_1}\sin\left(\lambda_j\frac{x}{L}\right) + \cosh\left(\lambda_j\frac{x}{L}\right) - \cos\left(\lambda_j\frac{x}{L}\right) - \sigma_j\left[\sinh\left(\lambda_j\frac{x}{L}\right) - \sin\left(\lambda_j\frac{x}{L}\right)\right] \tag{28}$$

where α_1 (= k_1L/EJ) is the non-dimensional stiffness of the left-end spring, and σ_j is given by

$$\sigma_j = \frac{\cosh\lambda_j - \cos\lambda_j + 2\dfrac{\lambda_j}{\alpha_1}\sin\lambda_j}{\sinh\lambda_j - \sin\lambda_j} \tag{29}$$

The eigenvalue λ_j is the solution of the following transcendental equation (Appendix A)

$$\alpha_1\alpha_2(1-\cosh\lambda_j\cos\lambda_j) + 2\lambda_j^2\sinh\lambda_j\sin\lambda_j + \lambda_j(\alpha_1+\alpha_2)(\sin\lambda_j\cosh\lambda_j - \cos\lambda_j\sinh\lambda_j) = 0 \tag{30}$$

α_2 (= k_2L/EJ) being the non-dimensional stiffness of the right-end spring.

Considering a resonant harmonic load, the j-th principal coordinate can be expressed by Eq. (23), where the amplitude can be obtained substituting Eq. (28) into Eq. (24)

$$A_j(\tilde{t}) = \frac{F_0}{4M_j\omega_j^2(\xi_j^4 - \lambda_j^4\tilde{\Omega}_c^4)}\left\{\begin{array}{l}\left[\dfrac{2\lambda_j^2\tilde{\Omega}_c}{\alpha_1}(\xi_j^2 - \lambda_j^2\tilde{\Omega}_c^2) + 4\lambda_j^2\tilde{\Omega}_c^2(\xi_j + \lambda_j\sigma_j\tilde{\Omega}_c)\right]\exp(-\xi_j\tilde{t}) \\ \quad +(\xi_j - \lambda_j\tilde{\Omega}_c)(\xi_j^2 + \lambda_j^2\tilde{\Omega}_c^2)(\sigma_j - 1)\exp(\lambda_j\tilde{\Omega}_c\tilde{t}) \\ \quad -(\xi_j + \lambda_j\tilde{\Omega}_c)(\xi_j^2 + \lambda_j^2\tilde{\Omega}_c^2)(\sigma_j + 1)\exp(-\lambda_j\tilde{\Omega}_c\tilde{t}) \\ +2(\xi_j^2 - \lambda_j^2\tilde{\Omega}_c^2)\left[\left(\dfrac{2\lambda_j}{\alpha_1}\xi_j - \sigma_j\xi_j + \lambda_j\tilde{\Omega}_c\right)\sin(\lambda_j\tilde{\Omega}_c\tilde{t})\right. \\ \quad \left.+\left(\dfrac{2\lambda_j^2}{\alpha_1}\tilde{\Omega}_c + \xi_j + \lambda_j\sigma_j\tilde{\Omega}_c\right)\cos(\lambda_j\tilde{\Omega}_c\tilde{t})\right]\end{array}\right\} \tag{31}$$

Thus, the time derivative of the amplitude in Eq. (31) is given by

$$\frac{dA_j(\tilde{t})}{d\tilde{t}}=\frac{F_0\lambda_j\tilde{\Omega}_c}{4M_j\omega_j^2(\xi_j^4-\lambda^4\tilde{\Omega}_c^4)}\left\{\begin{array}{l}\left[\frac{4\lambda_j\xi_j}{\alpha_1}(\xi_j^2-\lambda_j^2\tilde{\Omega}_c^2)-4\lambda\xi_j\tilde{\Omega}_c(\xi_j+\lambda_j\sigma_j\tilde{\Omega}_c)\right]\exp(-\xi_j\tilde{t})\\ +(\xi_j-\lambda_j\tilde{\Omega}_c)(\xi_j^2+\lambda_j^2\tilde{\Omega}_c^2)(\sigma_j-1)\exp(\lambda_j\tilde{\Omega}_c\tilde{t})\\ +(\xi_j+\lambda_j\tilde{\Omega}_c)(\xi_j^2+\lambda_j^2\tilde{\Omega}_c^2)(\sigma_j+1)\exp(-\lambda_j\tilde{\Omega}_c\tilde{t})\\ -2(\xi_j^2-\lambda_j^2\tilde{\Omega}_c^2)\left[\begin{array}{l}\left(\frac{2\lambda_j}{\alpha_1}\xi_j+\sigma_j\xi_j-\lambda_j\tilde{\Omega}_c\right)\cos(\lambda_j\tilde{\Omega}_c\tilde{t})\\ +\left(\frac{2\lambda_j^2}{\alpha_1}\tilde{\Omega}_c+\xi_j+\lambda_j\sigma_j\tilde{\Omega}_c\right)\sin(\lambda_j\tilde{\Omega}_c\tilde{t})\end{array}\right]\end{array}\right\} \tag{32}$$

The non-dimensional time $\tilde{t}_{\max}$ at which the amplitude A_j reaches the maximum value can be obtained setting equal to zero the time derivative of the amplitude. Since the first three terms in Eq. (32) are numerically negligible with respect to the last one, $\tilde{t}_{\max}$ is approximately given by

$$\tilde{t}_{\max}\simeq\frac{1}{\lambda_j\tilde{\Omega}_c}\operatorname{atan}\left(\frac{-2\frac{\lambda_j}{\alpha_1}\xi_j+\lambda_j\tilde{\Omega}_c-\sigma_j\xi_j}{2\frac{\lambda_j^2}{\alpha_1}\tilde{\Omega}_c+\lambda_j\sigma_j\tilde{\Omega}_c+\xi_j}\right)+\frac{\pi}{\lambda_j\tilde{\Omega}_c} \tag{33}$$

Therefore, the DAF β (26) for a generic Euler-Bernoulli beam can be expressed in closed form as a function of two non-dimensional parameters, $\tilde{\Omega}_c$ and ξ_j

$$\beta=\frac{1}{4\left|\varphi_j\right|_{\max}(\xi_j^4-\lambda_j^4\tilde{\Omega}_c^4)}\left\{\begin{array}{l}\left[-\frac{2\lambda_j^2\tilde{\Omega}_c}{\alpha_1}(\xi_j^2-\lambda_j^2\tilde{\Omega}_c^2)+4\lambda_j^2\tilde{\Omega}_c^2(\xi_j+\lambda_j\sigma_j\tilde{\Omega}_c)\right]\exp(-\xi_j\tilde{t}_{\max})\\ +(\xi_j-\lambda_j\tilde{\Omega}_c)(\xi_j^2+\lambda_j^2\tilde{\Omega}_c^2)(\sigma_j-1)\exp(\lambda_j\tilde{\Omega}_c\tilde{t}_{\max})\\ -(\xi_j+\lambda_j\tilde{\Omega}_c)(\xi_j^2+\lambda_j^2\tilde{\Omega}_c^2)(\sigma_j+1)\exp(-\lambda_j\tilde{\Omega}_c\tilde{t}_{\max})\\ +2(\xi_j^2-\lambda_j^2\tilde{\Omega}_c^2)\left[\begin{array}{l}\left(-\frac{2\lambda_j}{\alpha_1}\xi_j-\sigma_j\xi_j+\lambda_j\tilde{\Omega}_c\right)\sin(\lambda_j\tilde{\Omega}_c\tilde{t}_{\max})\\ +\left(\frac{2\lambda_j^2}{\alpha_1}\tilde{\Omega}_c+\xi_j+\lambda_j\sigma_j\tilde{\Omega}_c\right)\cos(\lambda_j\tilde{\Omega}_c\tilde{t}_{\max})\end{array}\right]\end{array}\right\} \tag{34}$$

where $\tilde{t}_{\max}$ is given by Eq. (33). Substituting the explicit value (33) of the non-dimensional time $\tilde{t}_{\max}$ into Eq. (34), it is evident that the DAF β depends on the non-dimensional speed parameter $\tilde{\Omega}_c$ and on the damping ratio ξ_j.

Furthermore, substituting the DAF β into the TRF β^*, Eq. (27), the TRF can be expressed as a function of the ratio $\tilde{\Omega}_c/\xi_j$ as follows

$$\beta^* = \frac{1}{2\left|\varphi_j\right|_{\max}\left(1-\lambda_j^4\frac{\tilde{\Omega}_c^4}{\xi_j^4}\right)}\left\{\begin{array}{l}\left[-\frac{2\lambda_j^2}{\alpha_1}\frac{\tilde{\Omega}_c}{\xi_j}\left(1-\lambda_j^2\frac{\tilde{\Omega}_c^2}{\xi_j^2}\right)+4\lambda_j^2\frac{\tilde{\Omega}_c^2}{\xi_j^2}\left(1+\lambda_j\sigma_j\frac{\tilde{\Omega}_c}{\xi_j}\right)\right]\exp\left(-\frac{1}{\lambda_j}\frac{\xi_j}{\tilde{\Omega}_c}\delta\right)\\ +\left(1-\lambda_j\frac{\tilde{\Omega}_c}{\xi_j}\right)\left(1+\lambda_j^2\frac{\tilde{\Omega}_c^2}{\xi_j^2}\right)(\sigma_j-1)\exp(\delta)\\ -\left(1+\lambda_j\frac{\tilde{\Omega}_c}{\xi_j}\right)\left(1+\lambda_j^2\frac{\tilde{\Omega}_c^2}{\xi_j^2}\right)(\sigma_j+1)\exp(-\delta)\\ +2\left(1-\lambda_j^2\frac{\tilde{\Omega}_c^2}{\xi_j^2}\right)\left[\begin{array}{l}\left(-\frac{2\lambda_j}{\alpha_1}-\sigma_j+\lambda_j\frac{\tilde{\Omega}_c}{\xi_j}\right)\sin(\delta)\\ +\left(\frac{2\lambda_j^2}{\alpha_1}\frac{\tilde{\Omega}_c}{\xi_j}+1+\lambda_j\sigma_j\frac{\tilde{\Omega}_c}{\xi_j}\right)\cos(\delta)\end{array}\right]\end{array}\right\} \tag{35}$$

where δ is a function of the ratio $\tilde{\Omega}_c/\xi_j$ and it is given by

$$\delta = \delta\left(\frac{\tilde{\Omega}_c}{\xi_j}\right) \simeq \operatorname{atan}\left(\frac{-2\frac{\lambda_j}{\alpha_1}+\lambda_j\frac{\tilde{\Omega}_c}{\xi_j}-\sigma_j}{2\frac{\lambda_j^2}{\alpha_1}\frac{\tilde{\Omega}_c}{\xi_j}+\lambda_j\sigma_j\frac{\tilde{\Omega}_c}{\xi_j}+1}\right) \tag{36}$$

In order to analyse the general tendency of the dynamic amplification on varying the involved non-dimensional parameters, Fig. 3 shows a surface plot of the DAF β for a simply-supported beam ($\alpha_1 = \alpha_2 = 0$) crossed by a harmonic load in resonance with the first mode of vibration, as a function of the damping ratio ξ_j and of the non-dimensional speed parameter $\tilde{\Omega}_c$: the DAF rapidly decreases on increasing both the damping ratio ξ_j and the non-dimensional speed parameter $\tilde{\Omega}_c$. It should be

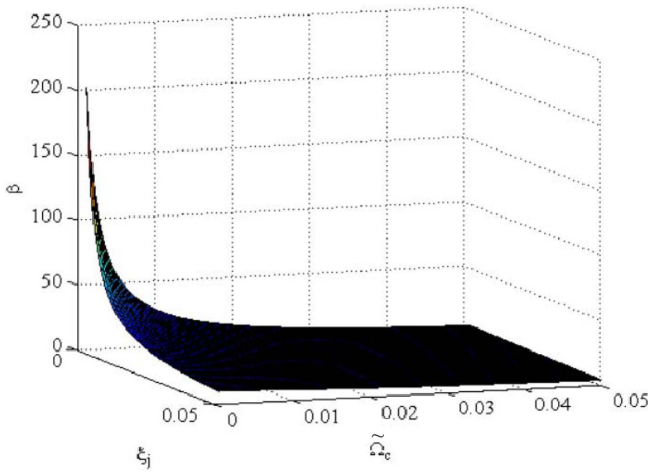

Fig. 3 Dynamic amplification factor β for a simply-supported beam crossed by a harmonic load in resonance with the first mode of vibration

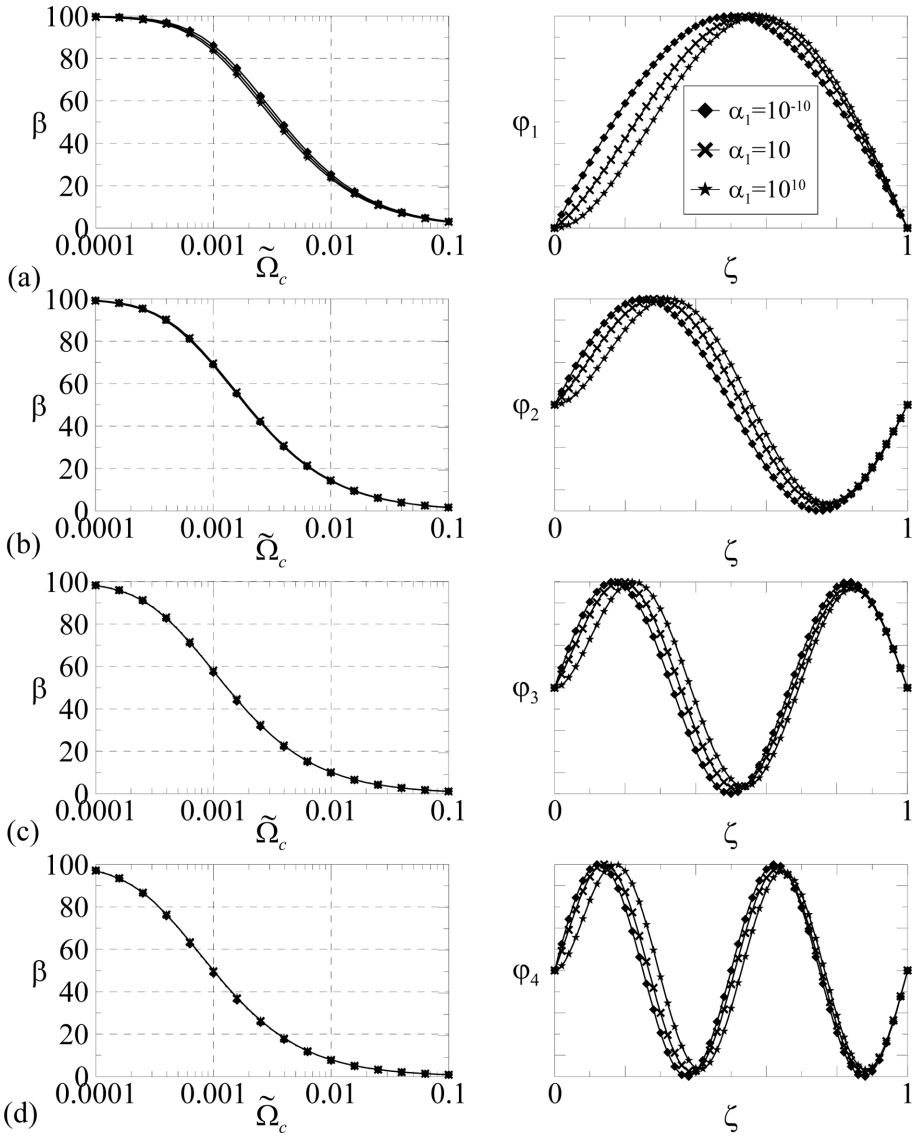

Fig. 4 Dynamic Amplification Factor β: $\alpha_2 = 0$, $\alpha_1 = 0, 10, \infty$: (a) $j = 1$, (b) $j = 2$, (c) $j = 3$, (d) $j = 4$ ($\xi_j = 0.005$)

pointed out that the closed-form solution here reported is reliable only when the non-dimensional speed parameter $\tilde{\Omega}_c$ is sufficiently small, $\tilde{\Omega}_c < 0.1$. This condition is easily satisfied if the velocity of the harmonic resonant load is small enough, as in the case of pedestrian-induced loading (e.g., Piccardo and Tubino 2012). If the harmonic load derives from the movement of train axles, $\tilde{\Omega}_c = 0.1$ corresponds to a load velocity $c \cong 0.3 \cdot c_{cr}$, being c_{cr} the critical speed of the bridge. For instance, for a trial bridge with a span of 30 m and a fundamental frequency of 3 Hz (Garinei 2006), $\tilde{\Omega}_c = 0.1$ corresponds to a load velocity $c = 56$ m/s, i.e. approximately 205 km/h. Thus, the closed-form solution here proposed is not reliable for very high speed loads.

In order to analyze the dependence of the DAF β on boundary conditions, Fig. 4 plots β as a

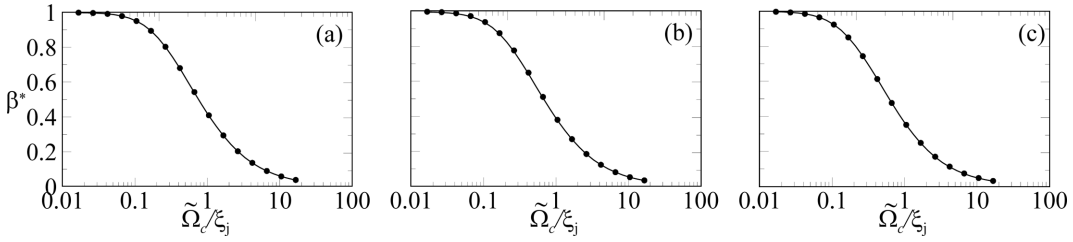

Fig. 5 Transition Deamplification Factor β^*: comparison between closed-form solution (solid line) and numerical solution (circles), (a) simply-supported, (b) pinned-clamped, (c) double-clamped

function of the non-dimensional speed parameter $\tilde{\Omega}_c$ (setting a modal damping $\xi_j = 0.005$), for a beam pinned at the right-hand side ($\alpha_2 = 0$) and for three different boundary conditions at the left-hand side: the pinned ($\alpha_1 = 0$) support, an intermediate situation ($\alpha_1 = 10$) and the perfect clamped ($\alpha_1 = \infty$) condition. The beam is crossed by a harmonic load in resonance with the j-th mode of vibration: (a) $j = 1$, (b) $j = 2$, (c) $j = 3$, (d) $j = 4$; right-hand figures show the shape of the corresponding vibration mode. The different boundary conditions clearly affect the DAF of the first vibration mode only, at low values of the non-dimensional speed parameter, Fig. 4(a), where the different left support leads to moderate differences (e.g., β changes from 86 to 83 when $\tilde{\Omega}_c$ = 0.001). When the non-dimensional speed parameter is increasing, or for higher modes, the DAF values seem not modified by the different boundary conditions. On the other hand, for a fixed value of the non-dimensional speed parameter (for instance, $\tilde{\Omega}_c = 0.001$), the DAF β is highly influenced by the vibration mode wherewith the harmonic load is resonant, showing a drastic reduction of the DAF on increasing the mode number (e.g., assuming $\tilde{\Omega}_c = 0.001$ and considering the simply-supported beam, $\beta = 86$ for the first mode, $j = 1$, and $\beta = 48$ for the fourth mode, $j = 4$).

Concerning the first vibration mode, Fig. 5 plots the analytical expression of the TDF β^*, Eq. (35), for three different boundary conditions, compared with its numerical values obtained through a direct use of the convolution Eq. (9). The proposed analytical solution appears very close to numerical values for all the support conditions, at least in the range of the ratio $\tilde{\Omega}_c/\xi_j$ considered in the Figure. In fact, as discussed above, the proposed solution is based on the assumption that $\tilde{\Omega}_c$ is small ($\tilde{\Omega}_c < 0.1$), therefore the ratio $\tilde{\Omega}_c/\xi_j$, ξ_j being small of the same order as $\tilde{\Omega}_c$, can not overcome values about 10. For higher values of the ratio $\tilde{\Omega}_c/\xi_j$, the analytical solution is not reliable and the maximum response often appears during beam's free vibrations.

In any case, it seems important to highlight that the limit value of the TDF β^* is not zero (i.e., the dynamic response is not nil) when the ratio $\tilde{\Omega}_c/\xi_j$ is increasing. Such a circumstance is due to the fact that, when $\tilde{\Omega}_c/\xi_j$ is high (i.e., the speed of the harmonic load is high and/or the damping ratio is very small) the deamplification due to the motion of the resonant harmonic load is very marked, and the dynamic response is approaching the maximum static response.

Fig. 6 summarizes the results of this Section comparing the TDF β^* for the three ideal support conditions of Euler-Bernoulli beams. Remarkable differences may be noted for intermediate values of the ratio $\tilde{\Omega}_c/\xi_j$; for instance, when $\tilde{\Omega}_c/\xi_j = 1$, the TDF assumes the value 0.41 for simply-supported beam and 0.35 for double-clamped beam, with a difference of about 17% in the maximum of the dynamic response.

The closed-form solution proposed in this Section can be easily adopted for any value of the stiffness of the springs at the ends of the beam (Appendix A). However, the expression of the mode

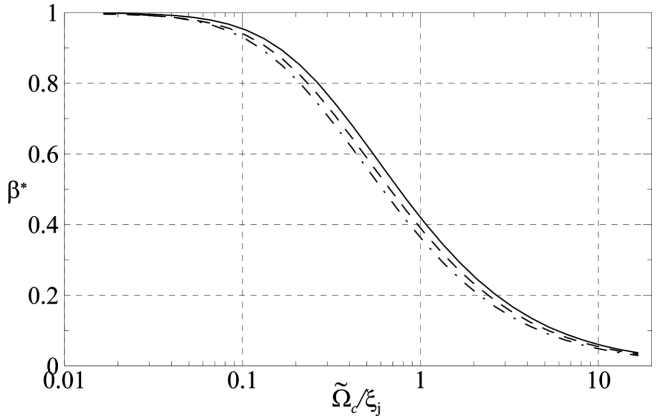

Fig. 6 Transition Deamplification Factor β^*: — simply-supported, – – pinned-clamped, – • – double-clamped

shape and the closed-form solution for the response amplitude and for the dynamic factors result considerably simplified when the stiffness of the supporting springs tend to zero (simply-supported beam) or to infinity (clamped beam). Section 3.1 and Section 3.2 illustrate the solution for the simply-supported beam and for the double-clamped beam, respectively.

3.1 Simply-supported beams

The solution for the simply-supported beam can be obtained from Eqs. (28), (31), (33), (34) and (35), setting $\alpha_1 = \alpha_2 = 0$.

In such a case, the j-th mode shape, Eq. (28), assumes the well-known form

$$\varphi_j(x) = \sin\left(j\pi\frac{x}{L}\right) \tag{37}$$

The amplitude of the j-th principal coordinate, Eq. (31), is given by

$$A_j(\tilde{t}) = \frac{F_0}{2M_j\omega_j^2(j^2\pi^2\tilde{\Omega}_c^2+\xi_j^2)}\left[-j\pi\tilde{\Omega}_c\exp(-\xi_j\tilde{t}) + j\pi\tilde{\Omega}_c\cos(j\pi\tilde{\Omega}_c\tilde{t}) - \xi_j\sin(j\pi\tilde{\Omega}_c\tilde{t})\right] \tag{38}$$

The non-dimensional time $\tilde{t}_{\max}$ at which the amplitude A_j reaches the maximum value, Eq. (33), becomes

$$\tilde{t}_{\max} = \frac{1}{j\pi\tilde{\Omega}_c}\left[\operatorname{atan}\left(-\frac{\xi_j}{j\pi\tilde{\Omega}_c}\right)+\pi\right] \tag{39}$$

Thus, the DAF β, Eq. (34), can be expressed as

$$\beta = \frac{1}{2(j^2\pi^2\tilde{\Omega}_c^2+\xi_j^2)}\left[-j\pi\tilde{\Omega}_c\exp(-\xi_j\tilde{t}_{\max}) + j\pi\tilde{\Omega}_c\cos(j\pi\tilde{\Omega}_c\tilde{t}_{\max}) - \xi_j\sin(j\pi\tilde{\Omega}_c\tilde{t}_{\max})\right] \tag{40}$$

where $\tilde{t}_{\max}$ is given by Eq. (39).

Finally, the TDF β^*, Eq. (35), assumes the following explicit expression

$$\beta^* = \frac{1}{\left(j^2\pi^2\frac{\tilde{\Omega}_c^2}{\xi_j^2}+1\right)}\left\{\begin{array}{c} -j\pi\frac{\tilde{\Omega}_c}{\xi_j}\exp\left[-\frac{1}{j\pi}\frac{\xi_j}{\tilde{\Omega}_c}\left(\operatorname{atan}\left(-\frac{1}{j\pi}\frac{\xi_j}{\tilde{\Omega}_c}\right)+\pi\right)\right] \\ +j\pi\frac{\tilde{\Omega}_c}{\xi_j}\cos\left[\operatorname{atan}\left(-\frac{1}{j\pi}\frac{\xi_j}{\tilde{\Omega}_c}\right)+\pi\right]-\sin\left[\operatorname{atan}\left(-\frac{1}{j\pi}\frac{\xi_j}{\tilde{\Omega}_c}\right)+\pi\right] \end{array}\right\} \tag{41}$$

The solution obtained in this Section is very similar to solutions already reported in the scientific literature. A solution for the dynamic response of simply-supported beams crossed by a resonant moving harmonic force has been obtained by Fryba (1999) in a different way, solving the equation of motion through the Laplace-Carlson transformation. Fryba (1999) also proposed an expression for a dynamic coefficient, conceptually equivalent to the DAF β, as a function of the speed and damping parameters; however, this dynamic coefficient shows a poor accuracy in applications. The interpretation of the dynamic response as a harmonic with slow-varying amplitude, and a closed-form solution for the DAF, have been first introduced by the authors of the present paper (Tubino and Piccardo 2008, Piccardo and Tubino 2009). Ricciardelli and Briatico (2011) have obtained analogous expressions for the response amplitude (38), for the time instant (39) when the amplitude reaches its maximum, and for the TDF (41); nevertheless the range of validity of their analytical solution is not clearly delineated.

3.2 Double-clamped beams

The solution for double-clamped beams can be obtained from Eqs. (28), (31), (33) and (34), setting $\alpha_1 = \alpha_2 = \infty$.

In such a case, the j-th mode shape, Eq. (28), assumes the form

$$\varphi_j(x) = \cosh\left(\frac{\lambda_j x}{L}\right)-\cos\left(\frac{\lambda_j x}{L}\right)-\sigma_j\left[\sinh\left(\frac{\lambda_j x}{L}\right)-\sin\left(\frac{\lambda_j x}{L}\right)\right] \tag{42}$$

The amplitude of the j-th principal coordinate, Eq. (31), is given by

$$A_j(\tilde{t}) = -\frac{F_0}{4M_j\omega_j^2(\xi_j^4-\lambda^4\tilde{\Omega}_c^4)}\left\{\begin{array}{c} -4\lambda^2\tilde{\Omega}_c^2(\xi_j+\lambda_j\sigma_j\tilde{\Omega}_c)\exp(-\xi_j\tilde{t}) \\ -(\xi_j-\lambda_j\tilde{\Omega}_c)(\xi_j^2+\lambda_j^2\tilde{\Omega}_c^2)(\sigma_j-1)\exp(\lambda_j\tilde{\Omega}_c\tilde{t}) \\ +(\xi_j+\lambda_j\tilde{\Omega}_c)(\xi_j^2+\lambda_j^2\tilde{\Omega}_c^2)(\sigma_j+1)\exp(-\lambda_j\tilde{\Omega}_c\tilde{t}) \\ +2(\xi_j^2-\lambda_j^2\tilde{\Omega}_c^2)\left[(\sigma_j\xi_j-\lambda_j\tilde{\Omega}_c)\sin(\lambda_j\tilde{\Omega}_c\tilde{t})-(\xi_j+\lambda_j\sigma_j\tilde{\Omega}_c)\cos(\lambda_j\tilde{\Omega}_c\tilde{t})\right] \end{array}\right\} \tag{43}$$

The non-dimensional time $\tilde{t}_{\max}$ at which the amplitude A_j reaches the maximum value, Eq. (33), becomes

$$\tilde{t}_{\max} = \frac{1}{\lambda_j\tilde{\Omega}_c}\operatorname{atan}\left(\frac{\lambda_j\tilde{\Omega}_c-\sigma_j\xi_j}{\lambda_j\sigma_j\tilde{\Omega}_c+\xi_j}\right)+\frac{\pi}{\lambda_j\tilde{\Omega}_c} \tag{44}$$

Furthermore, the DAF β, Eq. (34), can be expressed as

$$\beta = -\frac{1}{4\left|\varphi_j\right|_{\max}(\xi_j^4 - \lambda^4\tilde{\Omega}_c^4)}\left\{\begin{array}{c} -4\lambda^2\tilde{\Omega}_c^2(\xi_j + \lambda_j\sigma_j\tilde{\Omega}_c)\exp(-\xi_j\tilde{t}_{\max}) \\ -(\xi_j - \lambda_j\tilde{\Omega}_c)(\xi_j^2 + \lambda_j^2\tilde{\Omega}_c^2)(\sigma_j - 1)\exp(\lambda_j\tilde{\Omega}_c\tilde{t}_{\max}) \\ +(\xi_j + \lambda_j\tilde{\Omega}_c)(\xi_j^2 + \lambda_j^2\tilde{\Omega}_c^2)(\sigma_j + 1)\exp(-\lambda_j\tilde{\Omega}_c\tilde{t}_{\max}) \\ +2(\xi_j^2 - \lambda_j^2\tilde{\Omega}_c^2)\left[\begin{array}{c}(\sigma_j\xi_j - \lambda_j\tilde{\Omega}_c)\sin(\lambda_j\tilde{\Omega}_c\tilde{t}_{\max}) \\ -(\xi_j + \lambda_j\sigma_j\tilde{\Omega}_c)\cos(\lambda_j\tilde{\Omega}_c\tilde{t}_{\max})\end{array}\right] \end{array}\right\} \tag{45}$$

where $\tilde{t}_{\max}$ is given by Eq. (44).

The TDF β^* for the double-clampled beam is not liable for particular reductions and it assumes an expression very similar to Eq. (35), related to generically-supported Euler-Bernoulli beams.

4. Numerical examples

In this Section, in order to illustrate the reliability both of the proposed closed-form solution in the evaluation of the maximum dynamic response, and of its applicability to real bridges, two typologies of examples are considered: simple beams for which closed-form solutions are specifically deduced (Section 4.1), and an example of a real cable-stayed bridge (Section 4.2). For each structural example, the dynamic response is first evaluated through a numerical integration of the equation of motion; then, the proposed formulation is applied to analytically estimate the dynamic response of the beam and its maximum value.

4.1 Closed-form solution for simple beams

In order to clarify the reliability of the proposed closed-form solution for the maximum dynamic response, let us consider, as a test case, a clamped-pinned beam characterized by $\alpha_1 = \infty$, $\alpha_2 = 0$. At

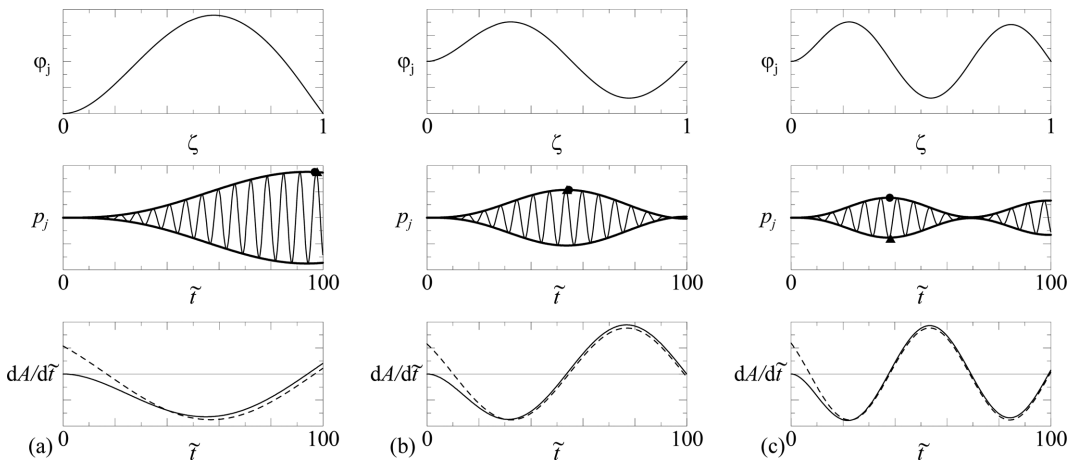

Fig. 7 Mode shape, time history of the principal coordinate, slow-varying amplitude and its time derivative for a simple beam: (a) $j = 1$, (b) $j = 2$, (c) $j = 3$

first, the dynamic response of the beam crossed by a harmonic moving load in resonance with one of the first three modes of vibration is evaluated, assuming the non-dimensional parameters $\xi_j = 0.005$, $\tilde{\Omega}_c = 0.01$ (Fig. 7). Then, the influence of the non-dimensional speed parameter on the dynamic response to a load in resonance with the first mode of vibration is investigated (Fig. 8).

The closed-form solution for the amplitude of the principal coordinate is given by Eq. (31), the time derivative of the amplitude is given by Eq. (32), the time at which the response is maximum by Eq. (33).

Fig. 7 shows the dynamic response of the beam to a load in resonance with one of the first three modes of vibration: (a) $j = 1$, (b) $j = 2$, (c) $j = 3$. The top figures show the beam mode shape. The middle figures show the time history of the j-th principal coordinate, comparing the numerical solution (thin solid line) with the closed-form solution proposed in this paper (dashed line), together with the closed-form amplitude (thick solid line). The triangle indicates the maximum numerical value of the principal coordinate; the circle denotes the maximum value provided by the closed-form solution proposed in this paper. The bottom figures represent the time derivative of the amplitude (solid lines), together with its approximation used in the evaluation of the maximum, obtained neglecting the first three terms in Eq. (32) (dashed lines).

From an inspection of the bottom figures, it can be deduced that the approximation of the time derivative of the response amplitude is very good in all the three modes; thus, the time at which the response amplitude is maximum is well estimated by the approximated closed-form solution. The middle figures show that the numerically-estimated time-histories of the principal coordinate are perfectly coincident with the analytical solutions (thin solid and dashed lines are not distinguishable); thus, the proposed closed-form solution practically coincides with the exact solution. The slow-varying amplitude of the principal coordinate p_j (solid thick lines) is able to perfectly envelope the time-varying response too. Thus, the maximum principal coordinate estimated analytically (circle) practically coincides with the numerically obtained maximum value (triangle). These results confirm the excellent precision of the proposed analytical solution in its validity domain, as already highlighted with reference to the TDF β^*, Fig. 5.

Concerning the first vibration mode ($j = 1$), Fig. 8 plots the time history of the principal coordinate for two different values of the non-dimensional speed parameter $\tilde{\Omega}_c$ ($\tilde{\Omega}_c = 0.001$, Fig. 8(a), $\tilde{\Omega}_c = 0.1$, Fig. 8(b)). When $\tilde{\Omega}_c$ is very small, Fig. 8(a), the proposed solution is surely valid and the dynamic response is optimally approximated by the proposed closed-form expression. In the limit case $\tilde{\Omega}_c = 0.1$, Fig. 8(b), the proposed solution still approximates well the dynamic response. As discussed in Section 3, the accuracy of the analytical solution tends to diminish when $\tilde{\Omega}_c$ becomes greater than 0.1. This occurs when the harmonic load performs few loading cycles during its permanence on the beam.

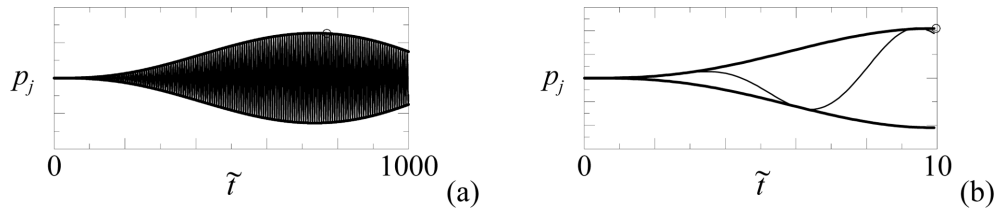

Fig. 8 Time history of the principal coordinate for a simple beam: (a) $\tilde{\Omega}_c = 0.001$, (b) $\tilde{\Omega}_c = 0.1$

4.2 Pedestrian-induced vibrations of a real cable-stayed bridge

In this Section, the pedestrian-induced dynamic response of a real cable-stayed footbridge is considered.

A single pedestrian walking on a footbridge exerts a dynamic loading in the vertical (v) and lateral (l) directions, $f_{pv}(t)$ and $f_{pl}(t)$, respectively, which can be schematized as periodic loading through a Fourier series (Allen and Murray 1993, Bachmann *et al.* 1995)

$$f_{pv}(t) = G + \sum_{i=1}^{n} G\alpha_{iv}\sin(2\pi i f_p t - \phi_i)$$

$$f_{pl}(t) = \sum_{i=1}^{n} G\alpha_{il}\sin(\pi i f_p t - \phi_i) \tag{46}$$

where G is the person's weight ($G \backsimeq 700$ N), α_{iv}, α_{il} are Fourier's coefficients (i.e., the dynamic load factors, DLFs) of the i-th harmonic in the vertical and lateral directions, respectively, f_p is the walking rate (Hz), ϕ_i is the phase shift of the i-th harmonic, i is the order number of the harmonic, n is the total number of contributing harmonics. For usual walking speeds, the frequency of the dominant harmonic is included between 1.6 and 2.4 Hz, and the DLF of the first vertical and lateral harmonics are $\alpha_{1v} \backsimeq 0.4$ and $\alpha_{1h} \backsimeq 0.1$, respectively (Bachmann *et al.* 1995, Zivanovic *et al.* 2005). Concerning the dynamic loading in the vertical direction, footbridges with natural frequencies below 5 Hz are considered as prone to human-induced vertical vibrations. A simplified vertical force model is given by a simple sinusoid in resonance with one structural mode of vibration (Fig. 1), moving across the bridge with a velocity c related to the pace frequency. Conventional Design Codes (see, e.g., FIB 2005) adopt such a simplifying loading model and require the classic evaluation of the maximum structural acceleration induced by the single pedestrian in order to verify bridge's vibration acceptability compared to suitable limit values.

The steel footbridge here considered has been recently built in Italy, and it is characterized by a

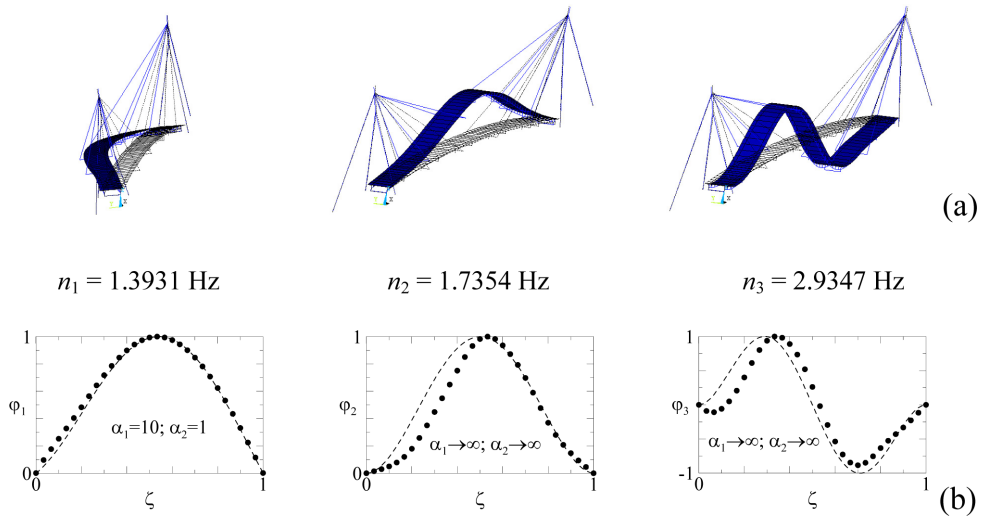

Fig. 9 Mode shapes of a real cable stayed bridge: (a) numerical results, (b) approximation with eigenfunctions of ideal Euler-Bernoulli beams

span length L = 59.37 m; it has been modelled by a finite-element code and a modal analysis has been performed, Fig. 9(a), subsequently verified through full-scale tests. The first mode of vibration (n_1 = 1.39 Hz) is flexural in the lateral direction, the second (n_2 = 1.73 Hz) and third (n_3 = 2.93 Hz) modes of vibration are flexural in the vertical direction. Fig. 9(b) shows the vibration modes obtained numerically (circle points) and their possible approximation through mode shapes of ideal Euler-Bernoulli beams (continuous lines). The proposed general procedure has been applied in order to evaluate the lateral/vertical dynamic response to a pedestrian crossing the bridge with a walking rate resonant with each of the first three modes of vibration; the results are compared with the response obtained by step-by-step dynamic analyses performed within the finite-element code. A modal damping $\xi_j = 0.005$ has been assumed for the first three modes of vibration, the sampling period is T_s = 0.01 s and the force amplitude has been assumed F_0 = 87.5 N for mode 1 (lateral direction) and $F_0 = 180$ N for modes 2, 3 (vertical direction). The velocity of the pedestrian is assumed c = 1.25 m/s for the analysis of mode 1, $c = 0.9 \times n_2$ = 1.56 m/s for mode 2, c = 2.5 m/s for mode 3.

Fig. 10 shows the time-histories of the numerically estimated accelerations (thin solid lines), compared with the solution proposed in this paper (dashed lines) in which the slow-varying

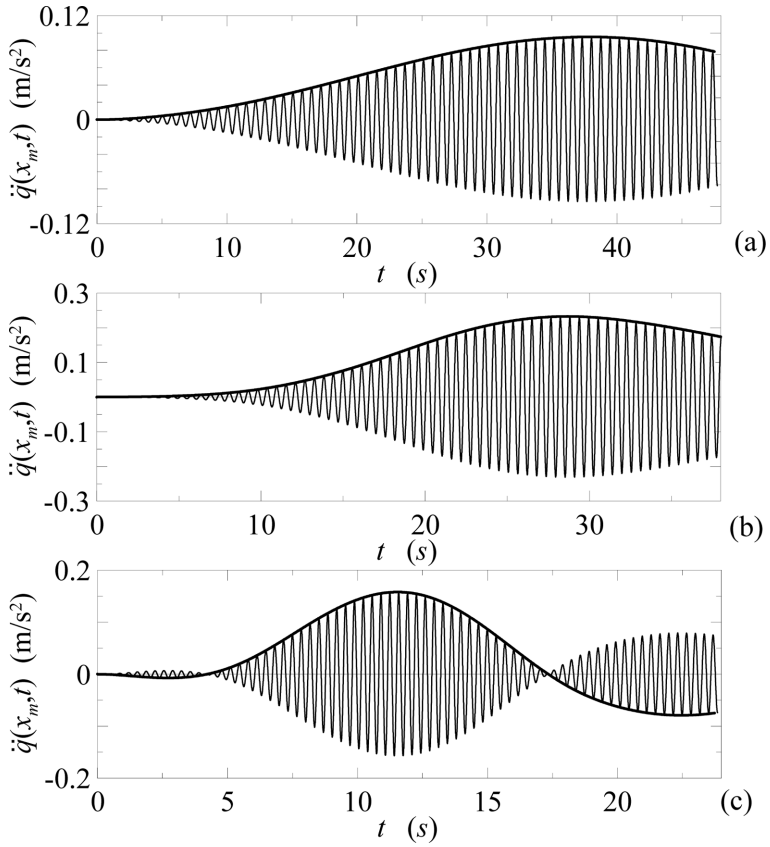

Fig. 10 Time-histories of acceleration for a real cable-stayed bridge: — step-by-step solution, – – proposed solution, — slow-varying amplitude), harmonic load resonant with the first (a), second (b) and third (c) mode of vibration

Table 1 Maximum dynamic response of a real cable-stayed bridge: comparison between the numerical results and the proposed closed form solutions for ideal Euler-Bernoulli beams

j	c (m/s)	$\ddot{q}_{\max}$ (m/s^2)	$\ddot{q}_{\max}$ (QS) (m/s^2)	$\tilde{\Omega}_c$	β	$\ddot{q}_{\max}$ (EB) (m/s^2)
1	1.25	0.095	0.0015	0.0024	61.8	0.093
2	1.56	0.23	0.0045	0.0024	57.1	0.256
3	2.5	0.16	0.0043	0.0023	41.5	0.176

amplitude is calculated from a discretization of the integral in Eq. (24) using the numerically-estimated modes (thick solid lines). Fig. 10(a) shows the lateral bridge acceleration at the deck mid-span ($x_m = L/2$) caused by a pedestrian walking in resonance with the first mode of vibration, Figs. 10(b) and 10(c) plot the vertical bridge acceleration to a pedestrian walking in resonance with the second and third mode of vibration, respectively, corresponding to the bridge deck abscissa x_m where the mode shape is maximum ($x_m = L/2$ for mode 2, $x_m \cong L/3$ for mode 3). In all the figures, thin solid and dashed lines are not distinguishable, thus, in all the cases analyzed, the response evaluated by the proposed method perfectly coincides with the response estimated by step-by-step analyses in finite-element codes. Moreover, the slow-varying amplitude (thick solid line) represents a perfect envelope of the solution. Therefore, the proposed general procedure, based on the representation of the response as a harmonic slowly modulated in time, confirms its applicability to generic footbridges and represents an efficient tool to estimate the maximum footbridge acceleration.

A further simplified analysis has been carried out in order to test the possibility of estimating the maximum acceleration induced by a walking pedestrian on a real footbridge, adopting the closed-form expressions for the DAF β (Section 3) with boundary conditions providing a good approximation of the numerical mode shapes. In particular, mode 1 can be considered as intermediate between the first mode shape of a pinned-pinned and a double-clamped beam, modes 2 and 3 are similar to the first and second mode shape of a double-clamped beam, Fig. 9(b). The numerical values for the stiffness of the supporting springs providing the selected approximation of the three mode shapes have been reported in the figure. The maximum acceleration of the real footbridge has been estimated multiplying the maximum quasi-static acceleration, $F_0 \varphi_{j\max}^2 / M_j$, and the DAF β for the approximating values of α_1 and α_2. Table 1 summarizes the results obtained for the 3 modes analyzed: column 2 reports the load velocity, column 3 quotes the maximum numerical acceleration estimated from the time-histories of Fig. 10, column 4 reports the maximum quasi-static acceleration, column 5 quotes the values of the non-dimensional frequencies $\tilde{\Omega}_c$, columns 6 and 7 report the corresponding values of the dynamic amplification factor and of the maximum acceleration evaluated adopting the proposed procedure. The comparison between the maximum accelerations evaluated from the time-histories (column 3) and the corresponding values estimated through the dynamic amplification factor for ideal Euler-Bernoulli beams (column 7) shows that the proposed analytical expressions for ideal beams is able to evaluate the maximum dynamic response of real complex structures with appreciable precision.

5. Conclusions

In this paper, the dynamic response of a Euler-Bernoulli beam crossed by a resonant harmonic

load moving with constant velocity has been found in closed-form, solving the equation of motion by a two-scale perturbation technique. It has also been shown that the same solution could be obtained by the convolution integral, neglecting small terms depending on the fast time-scale. The perturbation method points out the circumstance that the response can be modelled as a harmonic function with slow-varying amplitude, and suggests that the maximum response is achieved when this amplitude reaches its maximum value.

In case of Bernoulli-Euler beams with elastic rotational springs at the support points, starting from analytical expressions for the eigenfunctions, the time-history of the dynamic response and the Dynamic Amplification Factor have been provided in closed-form as functions of two non-dimensional parameters, the speed parameter and the damping ratio. A Transition Deamplification Factor is also introduced, depending only on the ratio between the speed parameter and the damping ratio. Such expressions appear of technical interest, since they allow the evaluation of the maximum dynamic response without the need for numerically made graphs, such as those proposed in the literature, or for step-by-step numerical analyses. The limits of validity of the proposed procedure have been deeply discussed as regards significant values of the non-dimensional parameters. For real bridges characterized by generic mode shapes, the maximum dynamic response can be evaluated adopting two different procedures: a first possibility is the (easy) discretization of the integral defining the slow-varying amplitude; the alternative is to seek an equivalent stiffness for the supporting springs in order to provide a reliable approximation of the structural mode shape, and to use the closed-form solution for ideal Euler-Bernoulli beams here proposed. Therefore, the proposed procedure represents an effective analytical tool for evaluating the sensitivity of a real bridge to vibrations induced by moving resonant harmonic loads.

Acknowledgments

This work has been partially supported by the Italian Ministry of Education, Universities and Research (MIUR) through the PRIN co-financed program “Dynamics, Stability and Control of Flexible Structures”.

References

Abu-Hilal, M. and Mosen, M. (2000), “Vibration of beams with general boundary conditions due to a moving harmonic load”, *J. Sound Vib.*, **232**(4), 703-717.

Allen, D.E. and Murray, T.M. (1993), “Design criterion for vibrations due to walking”, *AISC Eng. J.*, Fourth Quarter, 117-129.

Bachmann, H., Pretlove, A.J. and Rainer, H. (1995), “Dynamic forces from rhythmical human body motions”, *Vibration Problems in Structures: Practical Guidelines*, Birkhauser, Basel.

Catal, S. (2012), “Response of forced Euler-Bernoulli beams using differential transform method”, *Struct. Eng. Mech.,* **42**(1), 95-119.

Chen, Y.H., Huang, Y.H. and Shih, C.T. (2001), “Response of an infinite Timoshenko beam on a viscoelstic foundation to a harmonic moving load”, *J. Sound Vib.,* **241**(5), 809-824.

Clough, R.W. and Penzien, J. (2003), *Dynamics of Structures*, Third Edition, Computer & Structures Inc., Berkeley, CA, USA.

FIB (2005), *Guidelines for the Design of Footbridges*, Bulletin 32, International Federation for Structural Concrete, Lausanne, Switzerland.

Fryba, L. (1999), *Vibration of Solids and Structures Under Moving Loads*, Thomas Telford, London, UK.
Garinei, A. (2006), "Vibrations of simple beam-like modelled bridge under harmonic moving loads", *Int. J. Eng. Sci.,* **22**, 778-787.
Garinei, A. and Risitano, G. (2008), "Vibrations of railway bridges for high speed trains under moving loads varying in time", *Eng. Struct.*, **30**, 724-732.
Kargarnovin, M.H., Younesian, D., Thompson, D.J. and Jones, C.J.C. (2005), "Response of beams on nonlinear viscoelastic foundations to harmonic moving loads", *Comput. Struct.*, **83**, 1865-1877.
Kevorkian, J. and Cole, J.D. (1981), *Perturbation Methods in Applied Mathematics*, Springer-Verlag Inc., New York, USA.
Kim, S.M. (2004), "Vibration and stability of axial loaded beams on elastic foundation under moving harmonic loads", *Eng. Struct.*, **26**, 95-105.
Kocaturk, T. and Simsek, M. (2006), "Vibration of viscoelastic beams subjected to an eccentric compressive force and a concentrated moving harmonic force", *J. Sound Vib.,* **29**, 302-322.
Meirovitch, L. (1980), *Computational Methods in Structural Dynamics*, Sijthoff & Noordhoff, Alphen aan den Rijn, The Netherlands.
Nayfeh, A.H. and Mook, D.T. (1979), *Nonlinear Oscillations*, John Wiley & Sons, New York, USA.
Newmark, N.M. and Veletsos, A.S. (1952), "A simple approximation for the natural frequencies of partly restrained bars", *J. Appl. Mech.*, **19**, 563.
Oniszczuk, Z. (2003), "Forced transverse vibrations of an elastically connected complex simply-supported double-beam system", *J. Sound Vib.*, **264**, 273-286.
Piccardo, G. and Tubino, F. (2009), "Simplified procedures for vibration serviceability analysis of footbridges subjected to realistic walking loads", *Comput. Struct.*, **87**(13-14), 890-903.
Piccardo, G. and Tubino, F. (2012), "Equivalent spectral model and maximum dynamic response for the serviceability analysis of footbridges", *Eng. Struct.*, **40**, 445-456.
Pimentel, R. and Fernandes, H. (2002), "A simplified formulation for vibration serviceability of footbridges", *Proc. Int. Conf. on the Design and Dynamic Behaviour of Footbridges* (CD), Paris, France.
Rao, C.K. and Mirza, S. (1989), "A note on vibrations of generally restrained beams", *J. Sound Vib.*, **130**(3), 453-465.
Ricciardelli, F. and Briatico, C. (2011), "Transient response of supported beams to moving forces with sinusoidal time variation", *J. Eng. Mech., ASCE*, **137**(6), 422-430.
Simmonds, J.G. and Mann, J.E. Jr. (1998), *A First Look at Perturbation Theory*, 2nd Edition, Dover Publications, Inc., Mineola, N.Y.
Tubino, F. and Piccardo, G. (2008), "Vibration serviceability of footbridges: a closed-form solution", *Proc. Footbridge 2008, Third International Conference*, Porto, July.
Zivanovic, S., Pavic, A. and Reynolds, P. (2005), "Vibration serviceability of footbridges under human-induced excitation: a literature review", *J. Sound Vib.*, **279**, 1-74.

Appendix A

Let us consider an Euler-Bernoulli beam with elastically restrained ends, provided by rotational springs (Fig. 1). The equation of motion for free flexural undamped vibrations is

$$\mu \frac{\partial^2 q(x,t)}{\partial t^2} + EJ \frac{\partial^4 q(x,t)}{\partial x^4} = 0 \tag{47}$$

where $q(x, t)$ is the vertical/lateral displacement, EJ is the flexural stiffness, μ is the mass-per-unit-length.

The boundary conditions are given by (Fig. 1)

$$\begin{gathered} q(0,t) = 0 \\ EJ \left. \frac{\partial^2 q(x,t)}{\partial x^2} \right|_{x=0} = k_1 \left. \frac{\partial q(x,t)}{\partial x} \right|_{x=0} \\ q(L,t) = 0 \\ EJ \left. \frac{\partial^2 q(x,t)}{\partial x^2} \right|_{x=L} = -k_2 \left. \frac{\partial q(x,t)}{\partial x} \right|_{x=L} \end{gathered} \tag{48}$$

The natural modes of vibration can be found searching for solutions of Eq. (47) expressed as

$$q(x,t) = \varphi\left(\frac{x}{L}\right)\cos(\omega t) \tag{49}$$

Substituting Eq. (49) into Eq. (47), the mode shape $\varphi(x/L)$ has to satisfy the following differential equation

$$\varphi^{IV}\left(\frac{x}{L}\right) - \lambda^4 \varphi\left(\frac{x}{L}\right) = 0 \tag{50}$$

where λ is given by

$$\lambda^4 = \frac{\mu \omega^2 L^4}{EJ} \tag{51}$$

The general solution of Eq. (50) is given by

$$\varphi(x) = c_1 \sin\left(\lambda \frac{x}{L}\right) + c_2 \cos\left(\lambda \frac{x}{L}\right) + c_3 \sinh\left(\lambda \frac{x}{L}\right) + c_4 \cosh\left(\lambda \frac{x}{L}\right) \tag{52}$$

Imposing the boundary conditions, Eq. (48), the following system of equations is obtained

$$\begin{bmatrix} 0 & 1 & 0 & 1 \\ \alpha_1 & \lambda & \alpha_1 & -\lambda \\ \sin\lambda & \cos\lambda & \sinh\lambda & \cosh\lambda \\ -\lambda\sin\lambda + \alpha_2\cos\lambda & -\lambda\cos\lambda - \alpha_2\sin\lambda & \lambda\sinh\lambda + \alpha_2\cosh\lambda & \lambda\cosh\lambda + \alpha_2\sinh\lambda \end{bmatrix} \begin{Bmatrix} c_1 \\ c_2 \\ c_3 \\ c_4 \end{Bmatrix} = \begin{Bmatrix} 0 \\ 0 \\ 0 \\ 0 \end{Bmatrix} \tag{53}$$

Setting equal to zero the determinant of the coefficient matrix of the system (53), the following characteristic equation is obtained

$$-\alpha_2 + \cosh\lambda \left[\alpha_2 \cos\lambda - \frac{\alpha_1 + \alpha_2}{\alpha_1} \lambda \sin\lambda \right] + \lambda \sinh\lambda \left[\frac{\alpha_1 + \alpha_2}{\alpha_1} \cos\lambda - \frac{2\lambda_j}{\alpha_1} \sin\lambda \right] = 0 \tag{54}$$

An approximate solution for the frequencies of an elastically restrained beam has been reported by Newmark and Veletsos (1952), leading to

$$\lambda_j = \sqrt{\left[j + \frac{1}{2}\left(\frac{\alpha_1}{5j+\alpha_1}\right)\right]\left[j + \frac{1}{2}\left(\frac{\alpha_2}{5j+\alpha_2}\right)\right]}\,\pi \tag{55}$$

Furthermore, expressing the constants c_1, c_2 and c_3 as functions of c_4, the mode shape can be simply expressed as

$$\varphi(x) = \frac{2\lambda}{\alpha_1}\sin\left(\lambda\frac{x}{L}\right) + \cosh\left(\lambda\frac{x}{L}\right) - \cos\left(\lambda\frac{x}{L}\right) - \sigma\left[\sinh\left(\lambda\frac{x}{L}\right) - \sin\left(\lambda\frac{x}{L}\right)\right] \tag{56}$$

where σ is given by

$$\sigma = \frac{\cosh\lambda - \cos\lambda + 2\dfrac{\lambda}{\alpha_1}\sin\lambda}{\sinh\lambda - \sin\lambda} \tag{57}$$

Eq. (56) can be viewed as a particular case of the equation obtained by Rao and Mirza (1989), who analysed the more general case of a beam with both rotational and vertical springs at both ends, in the particular case when the stiffness of vertical springs tends to infinity.

The mode shape and characteristic equation for simply-supported and clamped beams can be obtained from Eqs. (54), (56) and (57) setting α_1 and α_2 equal to zero and infinity, respectively. The following Sections report the classic solution in such particular cases.

A.1 Simply-supported beam

In case of simply-supported beams, setting $\alpha_1 = \alpha_2 = 0$ in Eqs. (54) and (56), simplified expressions for the characteristic equation and for the mode shape can be obtained.

The characteristic equation can be expressed as

$$\sin\lambda = 0 \tag{58}$$

The mode shape becomes

$$\varphi(x) = \sin\left(\lambda\frac{x}{L}\right) \tag{59}$$

A.2 Clamped beam

In case of clamped beams, setting $\alpha_1 = \alpha_2 = \infty$ in Eqs. (54), (56) and (57), simplified expressions for the characteristic equation, for the mode shape and for the parameter σ can be obtained.

The characteristic equation can be expressed as

$$\cosh\lambda\cos\lambda = 1 \tag{60}$$

The mode shape becomes

$$\varphi(x) = \cosh\left(\lambda\frac{x}{L}\right) - \cos\left(\lambda\frac{x}{L}\right) - \sigma\left[\sinh\left(\lambda\frac{x}{L}\right) - \sin\left(\lambda\frac{x}{L}\right)\right] \tag{61}$$

Finally, σ is given by

$$\sigma = \frac{\cosh\lambda - \cos\lambda}{\sinh\lambda - \sin\lambda} \tag{62}$$